Ocean Engineering 309 (2024) 118541

Contents lists available at ScienceDirect

Ocean Engineering

journal homepage: www.elsevier.com/locate/oceaneng

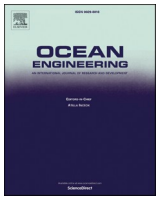

Research paper

Launch and recovery of a work class ROV through wave zone in small offshore service vessel

Yulin Deng [a], Xiudi Ren [b], Martin Nuernberg [c], Longbin Tao [a,*]

[a] Department of Naval Architecture, Ocean and Marine Engineering, University of Strathclyde, Glasgow, United Kingdom
[b] PowerChina Huadong Engineering Corporation Limited, Hangzhou, Zhejiang, China
[c] O.S.Energy (UK), Newcastle upon Tyne, United Kingdom

ARTICLE INFO

Keywords:
Offshore service vessel (OSV)
Remotely operated vehicle (ROV)
Snap load
Wave zone
Launch and recovery

ABSTRACT

The deployment of remotely operated underwater vehicle (ROV) from a small offshore service vessel (OSV) based on single point mooring system (SPMS) method is recently adopted in offshore renewable energy sector. However, the tension spike in wire, also known as snap load, often occurs when the ROV passes through the wave zone in launching and lifting operation of deployment. In this study, a practical numerical model for predicting wire tension during launch and recovery of ROV is developed and validated by wave flume test of a 1:10 scaled model. The numerical simulations reveal that the ROV deployment at vessel stern along with an appropriate reduction of horizontal distance from the hull are reliable safety strategies for reducing wire tension. By adopting the new deployment strategy, the annual operational capacity can be expanded by approximately 6% when the safe operational limit of ROV under a significant wave height of 1.25 m. Based on the comprehensive numerical simulation, the newly developed safe operating envelope provides a further guidance for onboard ROV operation in the O&M of offshore wind farms.

1. Introduction

During routine inspection and maintenance of potential scour, corrosion, welding and structural integrity of subsea vessel facilities, the majority of operators employ vessel and ROV based inspection methods. Large dynamic positioning (DP) vessels are commonly used to deploy ROVs in the oil and gas industry. The lack of suitable large offshore service vessels to perform regular inspections and maintenance of offshore wind farms is an obvious bottleneck with the rapid development of global offshore wind energy. Driven by the ongoing efforts of offshore renewable energy industry to reduce the levelized cost, the motivation for deploying ROVs using smaller vessels based on the Single Point Mooring System (SPMS) approach is evident (Nuernberg et al., 2021). The smaller vessel achieves a stable position by connecting to the wind turbine foundation via mooring lines to limit its movement in wind, waves, swells and currents. This allows the ROV to be deployed on the ship stern or side to conduct subsea inspections from a distance of approximately 30–45 m, as shown in Fig. 1. Larger ships do not significantly increase operating times even though they offer higher payload and stability in harsher environmental conditions. Moreover, the daily cost increase of a small ship is about one-tenth to one-fifth of the cost of large machinery required by a large ship. Another advantage of using smaller OSVs is the significant reduction in greenhouse gas emissions compared to the larger vessels used by conventional offshore O&G industry.

The ROV passes through wave zone from the initial position in the air and then reaches its working position in the water through the gradual extension of wire during the launch phase. During the recovery phase, the wire is gradually retracted to lift the ROV from underwater to original position after it has completed assigned tasks. Interactions between the ROV, ocean waves, and the support vessel can cause the wire to suddenly change from internal slack to taut state, significantly amplifying the tension experienced. Such occurrence, commonly referred to as snap load or sudden loading, may exceeds the specified safe working load or allowable strain leading to component damage. In contrast to large OSV operating in offshore O&G development, interaction between a small OSV and ROV in the field of combined wave and current sea-state can be significantly more complex. Therefore, a comprehensive analysis of ROV deployment procedures should be performed to determine the operational limits, taking into account nonlinear interactions between the ROV, wire, vessel, and wave dynamics.

* Corresponding author.
E-mail address: longbin.tao@strath.ac.uk (L. Tao).

https://doi.org/10.1016/j.oceaneng.2024.118541
Received 8 March 2024; Received in revised form 4 June 2024; Accepted 17 June 2024
Available online 20 June 2024

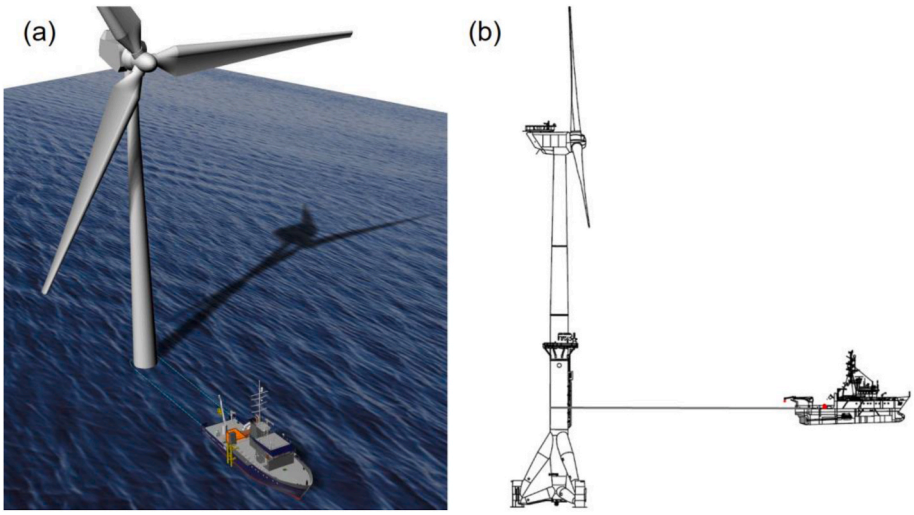

Fig. 1. 3D Model (a) and 2D Schematic (b) of ROV deployment in smaller vessel using SPMS method.

Table 1
Main dimensions of offshore support vessel – Fortuna Kingfisher.

Main dimensions	Vessel
Length overall (m)	38.92
Length waterline (m)	34.60
Length moulded (m)	32.10
Breadth moulded (m)	9.20
Depth (m)	4.50
Draught (m)	3.10
Displacement (m^3)	495.0
Lightship mass (t)	393

Table 2
Particulars of fixed offshore wind turbine.

Main dimensions	Wind turbine
Depth to platform base (m)	35
Height of tower (m)	120
Elevation to platform top (m)	10
Depth to top of taper (m)	4
Depth to bottom of taper (m)	12
Platform diameter above taper (m)	6.5
Platform diameter below taper (m)	9.4

Table 3
Properties of the whole work class ROV system.

Properties	TMS	ROV	ROV and TMS
Length (m)	1.792	1.515	1.792
Width (m)	1.491	0.790	1.491
Height (m)	2.317	1.0	2.317
Mass (kg)	1400	409	1809
Displacement (m^3)	0.394	0.401	0.795
Weight in water (kg)	996.2	0	996.2

Table 4
Properties of connecting lines.

Properties	Winch wire	Mooring line
Outer diameter (mm)	20.6	24.0
Weight in air (kg/m)	0.582	0.26
Weight in seawater (kg/m)	0.24	0.23
Axial stiffness (MN)	31.67	30.0
Bending stiffness (MN)	6.034	5.172
Max dynamic load (kN)	32.2	100.0

Table 5
Environmental data collected from weather forecast for the offshore operation.

Sea conditions	Properties	Values
Wind wave	Direction (deg)	330/SW
	Significant wave height (m)	0.5–1.25
	Peak periods (s)	3.0–5.0
Swell wave	Direction (deg)	40/SE
	Significant wave height (m)	0.2
	Peak periods (s)	4.5
Wind	Direction (deg)	330/SW
	Velocity (m/s)	5.4
Current	Direction (deg)	305/SW
	Velocity (m/s)	0.07–0.14

Table 6
The properties and coefficients of slender elements.

Properties	TMS	ROV	ROV and TMS
Porosity	0.94	0.67	0.87
Element number	39	26	65
Added mass coefficient	0.55	0.72	–
Linear drag coefficient	0.3	0.3	–
Quadratic drag coefficient	4.0	2.5	–

The launch and recovery process of an ROV is essentially a lifting operation with special emphasis on navigation in wave zones. Extensive research on modelling subsea lifting operations has been reported, covering numerous contributions over the past decades. (Lubis and Kimiaei, 2021; de Andrade et al., 2023) provided a review of the existing literature on operational phases and modelling related to lifting operations. The current recommended practices for lifting operation are primarily derived from the guidance provided by DNV (2019) and are commonly used as the main reference for operators and suppliers. The guidance offers a comprehensive approach and a simplified method to assessing all phases of subsea lifting operations including lifting off from the deck, manoeuvring from the vessel, lowering through the wave zone, descending to the seabed, and positioning and landing. However, some studies (Kimiaei et al., 2009; Valen, 2010) indicated that the DNVGL recommended practices often lead to overestimation of results by comparing the results from simplified method and numerical simulation.

The nonlinear relationship between waves and wire tension is difficult to accurately model through simple mathematical formulas because

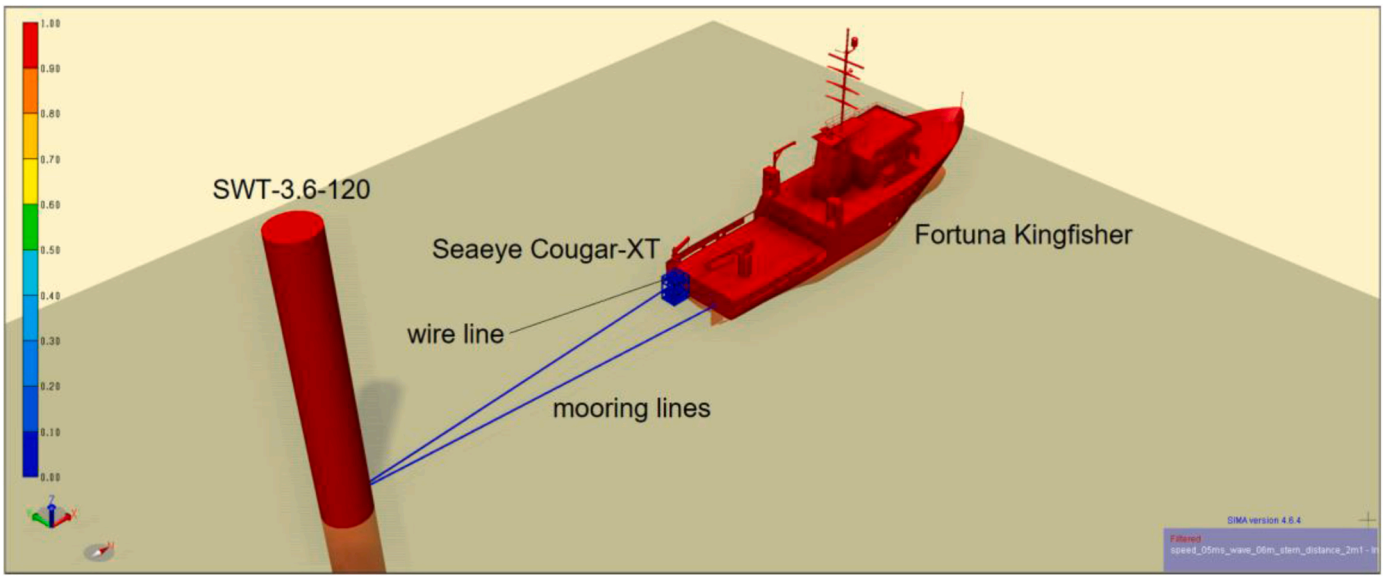

Fig. 2. Numerical simulation model of launching and recovering ROV in vessel stern in SIMA.

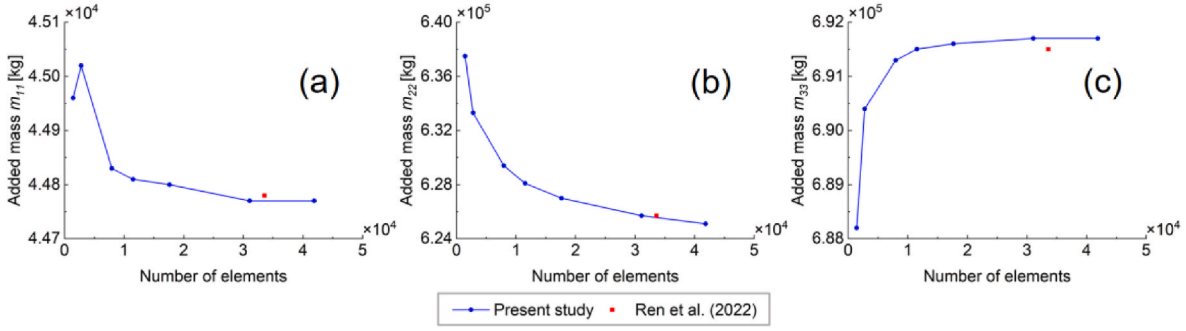

Fig. 3. Mesh convergence and validation of added mass in surge (a), sway (b) and heave (c) for hull model elements.

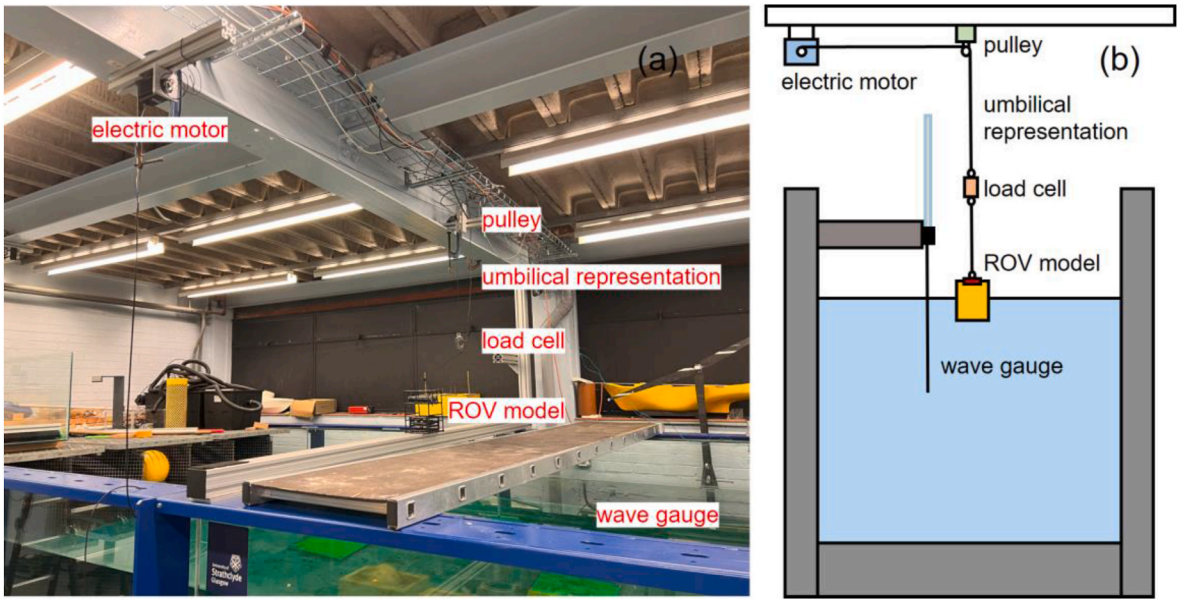

Fig. 4. Picture of field measurement (a) and sketch of experiment setup (b).

Table 7
Dimensions of ROV prototype, numerical and experimental model.

Dimensions	Prototype	Simulation	Experiment
Length (m)	1.792	1.792	0.18
Width (m)	1.491	1.491	0.15
Height (m)	2.317	2.317	0.23
Mass (m)	1809	1809	1.81
Displacement (m^3)	0.795	0.795	0.80×10^{-3}
Weight in water (kg)	996.2	996.2	1.00

of the wave impacts act on both ROV and ship simultaneously. Numerical simulation and experimental methods are currently used as the primary means of researching lifting operation. Driscoll et al. (2000) predicted the motions of a vertically tethered cage ROV system, and the tension of onboard tethers based on a one-dimensional finite element lumped mass model excited by surface waves. A numerical scheme to evaluate the effect of communication cables attached to underwater vehicles was proposed by Feng and Allen (2004). The interaction between ROV and offshore system has been captured in several studies by conducting scaled experiments in wave tank. Sayer (2008) measured the added mass and drag coefficient of a work class ROV passing through the wave zone by performing experiments in a wave flume using a 1:8 scale model. Some measures to eliminate or reduce transient loads on wire were provided by Lubis (2021) in a study on the dynamic tensile loading of an ultra-deepwater ROV under the combined effect of waves and ship motion. The ship motion was simplified to simple harmonic motion in tests and regular waves were used for environmental simulation. Relaxation and tension test of connecting wire is another more direct method of studying transient loads. Hennessey et al. (2005) proposed a mathematical model of rope force as a function of weight displacement and velocity when a slack rope is tightened by performing static and dynamic tests of 11 synthetic ropes. Hsu et al. (2017) measured the effect of sudden loading on mooring lines consisting of stainless-steel chains in shallow water by conducting transient load experiments in a wave pool.

In this study, a practical numerical model for predicting wire tension is developed for a work class ROV passes through the wave zone during launch and recovery from a small OSV. Weather forecast data of waves, swells, winds and currents for the DanTysk wind farm located in the North Sea are used to simulate realistic operating sea conditions. The developed model is validated against experimental test results of calm water and regular waves on a 1:10 scaled model in a wave flume. Various combinations of key factors including winch speed, waves, ship motion and deployment positions are studied for their effects on the magnitude of snap load in detail. Based on the comprehensive parametric analysis, a new multi-parameter criterion is proposed to determine the environmental limit for safe operation of the working ROV on board a small OSV. Finally, a safe operational window for the work class ROV deployed from the small vessel is determined to navigate the wave zone during launch and recovery procedure.

2. Numerical model development

2.1. Offshore service vessel and wind turbine

The existing offshore support vessel known as the Fortuna Kingfisher has been conducting foundation inspection of offshore wind farms using ROV during the last five years. Its primary characteristics are detailed in Table 1. The data and a panel model of the OSV Fortuna Kingfisher have been provided by O.S. Energy Ltd.

The offshore wind turbine for this project is a mono-pile bottom fixed wind turbine located at the DanTysk wind farm. It is a Siemens SWT-3.6-120 Offshore with a tripod support structure. Its further details are shown in Table 2.

2.2. ROV and TMS system

The offshore support vessel is equipped with an ROV called Seaeye Cougar-XT and specially retrofitted to perform inspection, maintenance, and repair work on facilities located below the water surface. A whole work class ROV system contains ROV and tether management system (TMS) type 8. The ROV remains connected to the TMS during the deployment procedure and detaches from the TMS during the operational phase. The primary characteristics of the entire system can be found in Table 3. The ROV and TMS system are collectively called ROV for simplicity in this study.

2.3. Winch wire and mooring lines

The single rope/mooring line to restrain motion of the vessel at a fixed radius around the foundation of wind turbine is a 3-strand Superflex polyester rope. The winch wire used for launch and recovery of ROV is a 20 mm single mode tether. The data of connecting lines are acquired from Randers Reb and Bridon Bekaert company, as shown in Table 4.

2.4. Sea conditions of the DanTysk wind farm

The DanTysk is a 288-MW offshore wind farm in the North Sea 70 km west of the island Sylt. The data of sea conditions for the DanTysk wind farm are derived from the 2020 StormGeo weather forecast during regular seabed inspection, as shown in Table 5.

Table 8
Experimental test conditions of regular waves.

Water	Conditions	Prototype	Simulation	Experiment
Calm water	Winch speed (m/s)	0.5	0.5	0.16
Regular waves	Wave height (m)	0.60	0.60	0.06
	Wave period (s)	7.03	7.03	2.22
	Winch speed (m/s)	0.5	0.5	0.16

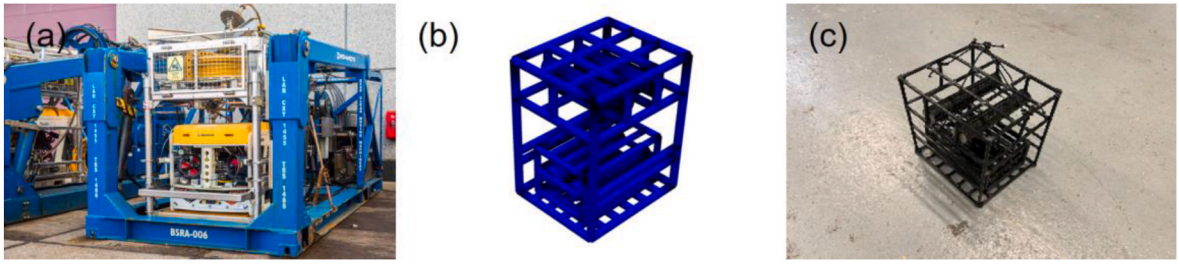

Fig. 5. Prototype (a), numerical model (b) and experimental model (c) of ROV.

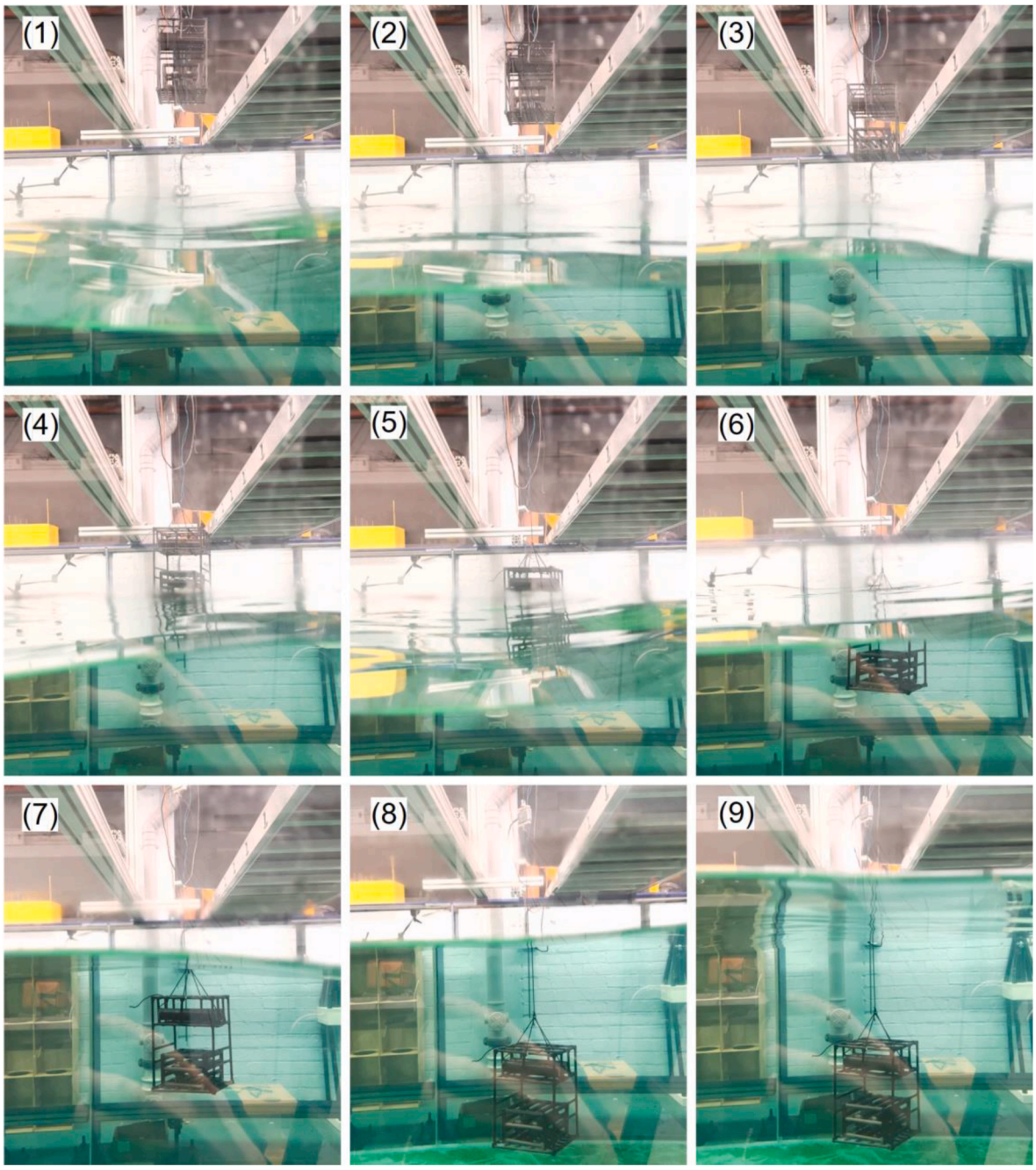

Fig. 6. Snapshots of ROV launch operation in regular waves.

2.5. Numerical model implementation, verification and validation

The operation of launching and recovering an ROV, a typical offshore crane operation, will be simulated using Hydrodynamic Analysis and Stability Analysis (HydroD) and Marine Operations and Mooring Analysis (SIMA) software developed by DNVGL in this study. HydroD is a software tool for frequency domain analysis of barges, ships and platforms with advanced wave load analysis options. SIMA is an advanced module for time domain simulation of the motion and position-keeping behaviour of complex marine structures, operations and floating systems.

The ROV can be represented by a simplified structural model consisting of slender elements recommended by the SIMO theory manual (SINTEF Ocean, 2022) due to limitations of available drawings and data. The numerical model of ROV is composed of 65 slender elements and its structural dimensions align with those listed in Table 3. The visualization of ROV is shown in Fig. 5. Certain hydrodynamic coefficients of ROV including added mass and drag coefficients must be provided as inputs to estimate the motion and response as it traverses the wave zone. However, these coefficients are challenging to determine, and there is a scarcity of information and data on ROV correlation coefficients. The added mass coefficients are determined with reference to the hydrodynamic problems in viscous flow of square prisms in the DNVGL recommended practice (bjerkholt, 2014; jenssen, 2015). the drag coefficients are based on the data of characteristic parameters describing the subsea structure in the investigation of fluid dynamics of idealized complex objects from øritsland (1989). the roV is a neutrally buoyant floating body with approximately equal gravity and buoyancy, and the TMS is described as a container carrier module with more gravity than buoyancy but with relatively insignificant excess mass in the Øritsland and

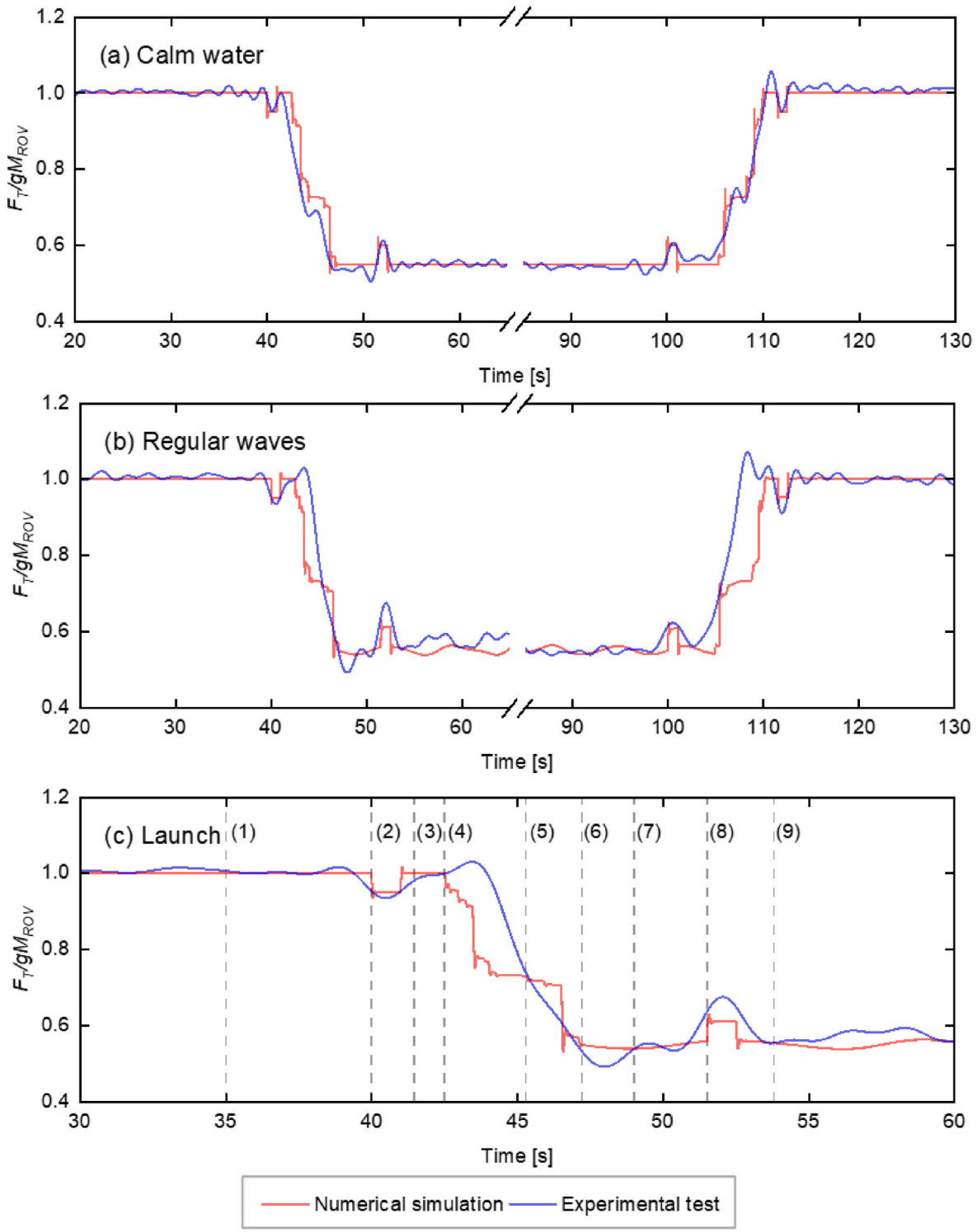

Fig. 7. Comparison of dynamic tensions in wire from simulation and test in calm water (a), regular waves (b) and launch phase in regular waves (c).

Lehn study. The final estimated hydrodynamic coefficients of the ROV model are displayed in Table 6.

The crane tip is modelled as a unified body point integrated with the winch. The motion and response of crane tip are represented by response amplitude operator (RAO) of vessel in frequency domain analysis. The vessel RAO is calculated by HydroD and then imported into SIMA for coupling time domain analysis. The wind turbine has been simplified to a simple cylinder and is simulated as a fixed mass body point. The winch wire is a separate model that connects the crane tip to the top of ROV and it is conceptualized as a simple wire coupling. Two identical mooring lines are modelled as the simple wire couplings used to connect the ship to the wind turbine. The time integration step and time increment are 0.005 s based on the convergence test.

The offshore vessel is located approximately 40 m in front of the wind turbine. The winch that extends and shortens the wire is represented by a crane tip located 5.0 m above the free water surface. The ROV top is connected to the winch by a wire and is located 0.7 m below the position of crane tip. The ROV will be lowered to a depth of 20.0 m

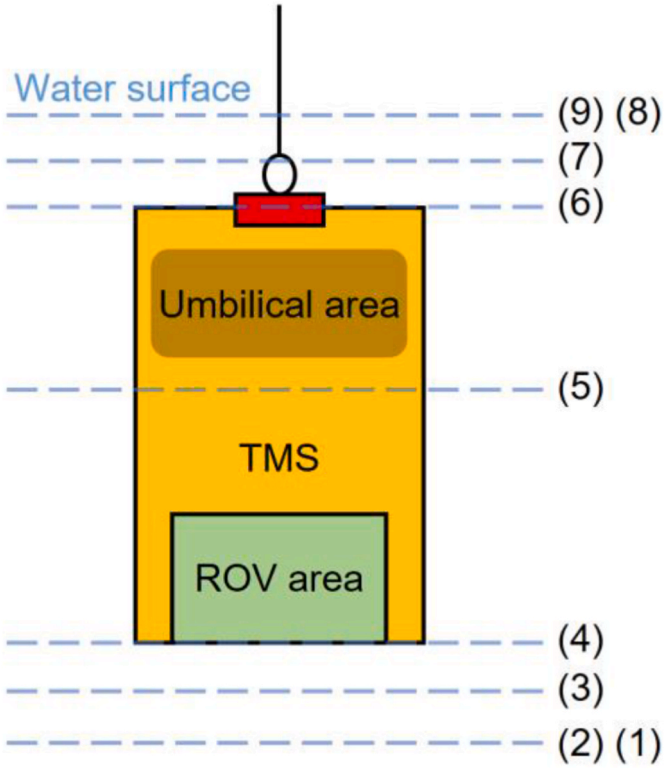

Fig. 8. The free water surface positions in ROV launch operation.

below the free surface at the set winch speed after the winch is started, and then the ROV will be lifted out of the water to its initial position at the same speed after the winch stops for a period of time representing the underwater work. The numerical simulation model of launching and recovering ROV is shown in Fig. 2.

The panel mesh for offshore vessel is needed since there are two bodies in the hydrodynamic interaction calculation. Fig. 3 shows the mesh convergence analysis for the case of headed waves and a wave frequency of 1.21 rad/s. The numerical result of added mass converges to the actual added mass value as the number of elements increases. Approximately 35,000 ship hull panel elements are sufficient to accurately estimate wave loads in the present case. Ren et al. (2022) conducted a study on the line tension between a fixed wind turbine and an offshore support vessel in a similar single point mooring configuration. The service vessel employed in this study is consistent with that described in the existing literature. The validity of the numerical model is further strengthened by comparison with added mass results in the literature. In Fig. 3, the red point is obtained from the literature results (Ren et al., 2022) and the blue curve represents the results of the present numerical simulation. Clearly, the close agreement indicates that the present numerical model is reliable.

3. Experimental campaign

3.1. Experimental setup and test procedure

The experiment is conducted in a wave flume at the Kelvin Hydrodynamics Laboratory, University of Strathclyde. An electric motor representing the crane tip motion and winch operation is mounted on a rigid frame 1.5 m above the water surface. Since it is impossible to obtain a wire consistent with the scaling parameters of the actual wire, a soft rope with low bending stiffness was chosen for connecting the electric motor and the ROV model. The rope is supported by a pulley mounted on the frame. A load cell is placed between the pulley and the ROV model to monitor and record the axial load in the wire representation. The tank is filled with fresh water to a depth of 1.1 m. The ROV is positioned at the midpoint of wave flume to access the area with stable wave condition. The wave generator on one side of the water tank generates the set waves, and a wave gauge is installed 0.5 m in front of the position of the ROV model to measure the wave characteristics and transformation. It is noteworthy that the experiment does not account for the motion of vessel. Similarly, in Section 3.2, the validation of the numerical simulation results excludes the ship's motion corresponding to the situation of the model tests. In the subsequent section of Chapter 4, the ship's motion is included in the numerical simulations for fully coupled analysis. The picture of field measurement and schematic of the experimental setup are shown in Fig. 4.

The experiment uses a 1:10 work class ROV model composed of several small cylinders. The parameters of the ROV prototype and model are shown in Table 7. The shape and volume of each cylinder are determined by the pultruded carbon fibre pipe shell, and the weight is determined by the inner core made of stainless-steel rods. The experiment model achieves the same properties as each slender element in the numerical simulation at the scale dimension. The ROV prototype, numerical model and experimental model are shown in Fig. 5. Launch and recovery operation tests are conducted in calm water and regular waves, and the time histories of wire tension are recorded. The wave height and period of regular waves are shown in Table 8.

3.2. Validation of numerical model

The experimental tests first simulated the launch procedure and then the recovery procedure. Due to the short initial distance between the bottom of ROV model and the water surface, the winch is suddenly activated at a selected speed excluding an acceleration procedure. Sudden changes in winch speed when starting and stopping inevitably result in brief fluctuations in wire tension that disappear after a certain duration. Fig. 6 shows a set of snapshots of ROV launch test in regular waves. The ship motion in numerical simulation is removed by restraining six degrees of freedom of the hull to achieve conditions comparable to those in the experiment. The experimental test results at model scale are scaled up and compared with the numerical simulation results at full scale, as shown in Fig. 7. The experimental data are processed using a low-pass filter with a cutoff frequency of 2 Hz. The free water surface positions in ROV launch operation are shown in Fig. 8.

The serial numbers (1)–(9) represent the snapshot of the shooting moment of the ROV launch operation in regular waves in Fig. 6, the corresponding time instants in the dynamic tensions in the wire from the simulation and test results in Fig. 7(c), and the free water surface positions in the ROV launch operation in Fig. 8. By observing Figs. 6–8, the ROV initially remains stationary in air and the wire tension is equal to the object gravity in case as shown in Fig. 6(1). A sudden slack of wire occurs when the speed is transferred from the wire to the load cell after winch starts in Fig. 6(2) which causes a rapid reduction and then recovery of the tension. Fig. 6(3) represents the uniform linear motion of ROV in vertical direction in air. The bottom of the ROV touches the free water surface in Fig. 6(4) and the wire tension decreases with increasing buoyancy. The load components that make up the dynamic force are the slamming impact force from waves on the bottom of ROV and the inertial force. The slamming impact force is controlled by the relative velocity between the ROV and waves. Fig. 6(5) shows a slight decrease because the buoyancy volume change in middle section is smaller compared to the ROV storage area and wire storage area. The load components including drag force, mass force and inertial force act together on the ROV. The mass force is composed of the hydrodynamic mass of ROV submerged part and the acceleration of water particles. The ROV is fully submerged in Fig. 6(6), and then the ROV continues to move a certain distance in water represented by Fig. 6(7). The load components are drag forces and mass forces on the ROV. It is seen that the crane stops descending showing in Fig. 6(8) and a sudden increase in wire tension will occur due to the downward vertical inertia of ROV.

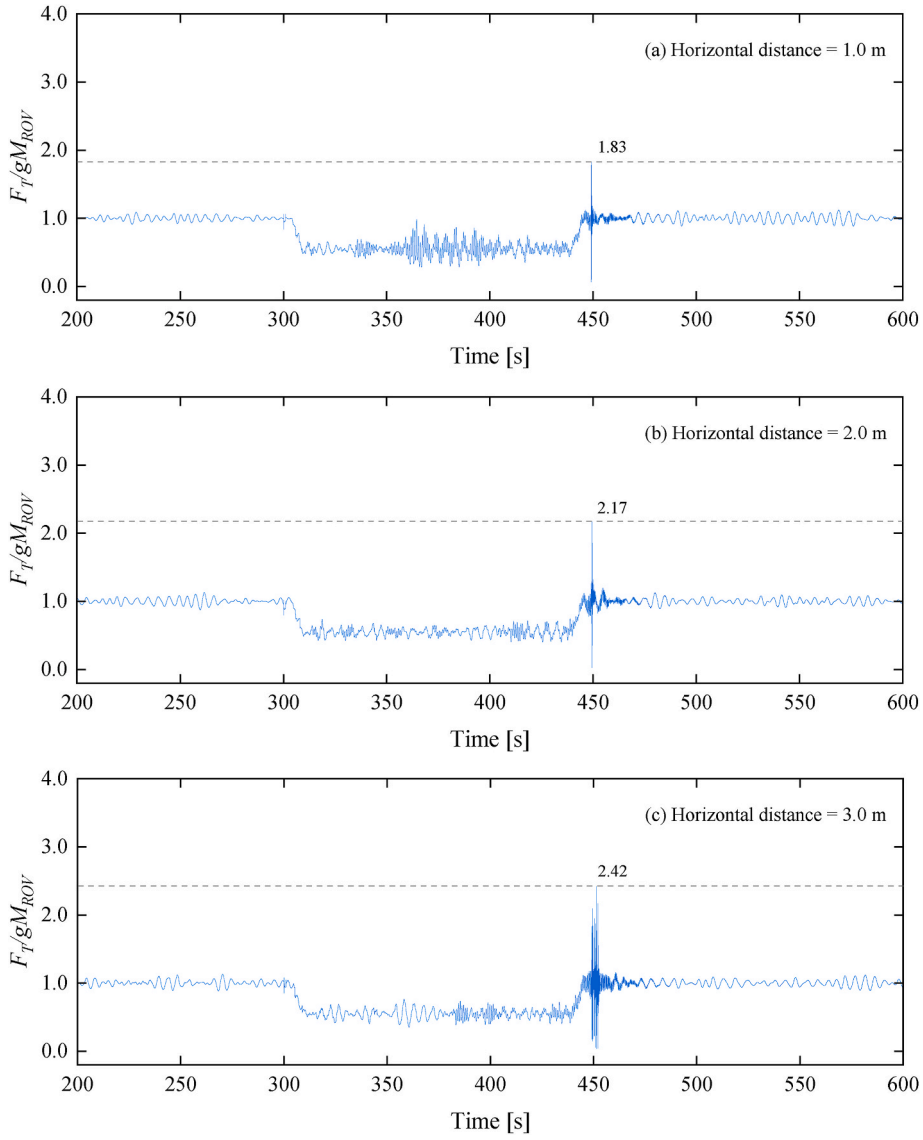

Fig. 9. Time history of wire tension during ROV deployment from vessel stern at three horizontal distances.

Finally, the launch procedure ends and the ROV stays in the working position represented by Fig. 6(9). The wire tension for the recovery procedure is reversed. The results of numerical simulation show a good agreement with experimental measurements with similar phase trend in Fig. 7, indicating that the present numerical model is reliable with high degree of accuracy.

4. Numerical simulation: small OSV operation capability – examination and capacity extension

Following the validation against the purposely conducted laboratory experiments of ROV launch and recovery process, and the results of the OSV vessel dynamics and the mooring tension from the previous numerical study (Ren et al., 2022), the present numerical model is applied to investigate the ROV operation onboard a small OSV using a single point mooring system. Numerical simulation is focused on factors crucial to the operation including effect of deployment position, influence of winch speed, and environmental limit to the ROV operation. Based on the detailed study, an improved ROV deployment strategy is recommended for expanding ROV operational capacity onboard a small OSV for offshore wind farms.

4.1. *Effect of deployment position*

The deployment position of ROV is situated either at the vessel side or stern, ensuring a specific horizontal distance from the hull. This minimum horizontal distance is typically set at half the ROV's length to prevent collisions during operational manoeuvrers, while the maximum distance from the hull is constrained by the crane boom's length. In this study, the ROV's launch location is positioned centrally between two mooring lines at the vessel stern. However, deployment on the ship side is sometimes necessitated due to obstructions from mooring lines. The crane arm can extend up to a maximum distance of 4.0 m. Fig. 9 shows the time history of wire tension at three horizontal distances from the vessel stern at the significant wave height 0.6 m and winch speed 0.5 m/s. Fig. 10 shows the simulation results of ROV being deployed on the ship side with different distance from the hull.

The peak wire tension is observed when the crane halts during the recovery phase when the ROV deployed at vessel stern, as illustrated in Fig. 9. This peak is due to the abrupt cessation of winch speed, leading to transient fluctuations in wire tension. These fluctuations are seen gradually subside over time. The maximum wire tension during the recovery phase is approximately 2.4 times higher than that during the launch phase for the same horizontal distance in Fig. 9(c). While the

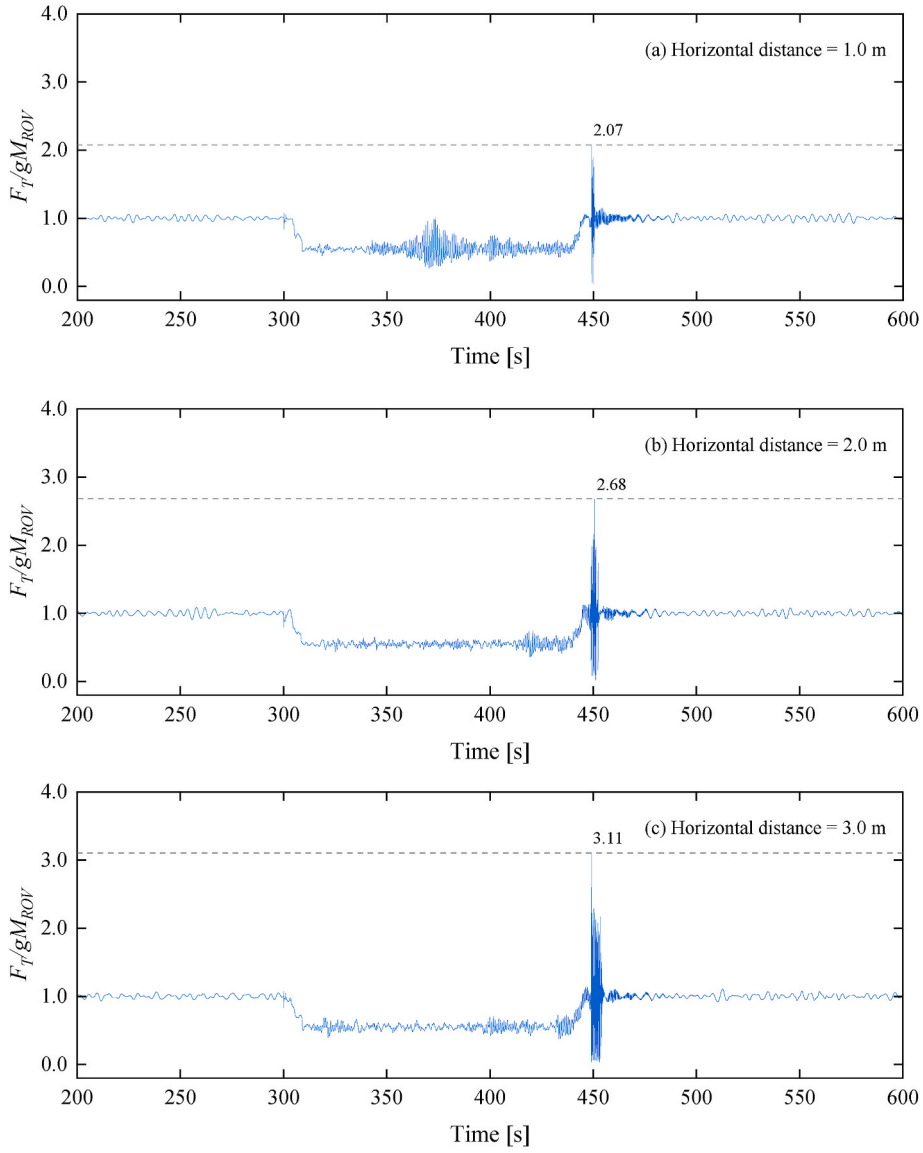

Fig. 10. Time history of wire tension during ROV deployment from vessel side at three horizontal distances.

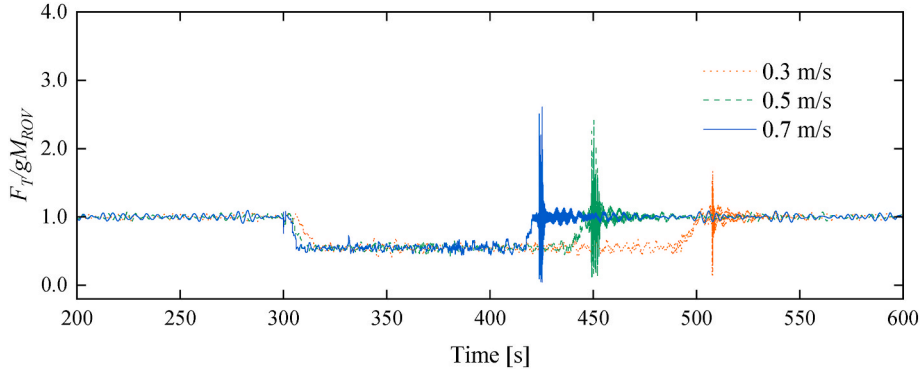

Fig. 11. Time history of wire tension for ROV deployment 2 m from vessel stern at three different winch speeds.

increase in horizontal distance marginally affects wire tension during the launch phase, its impact on the maximum wire tension during the recovery phase is evidently more significant. This can be attributed to the fact that the horizontal distance acts as a radius of gyration, amplifying the ROV's movement and momentum with increased distance, especially under the vessel heave acceleration and water particle movements. Therefore, opting for a deployment position with a shorter horizontal distance is advantageous while ensuring the safety of the equipment by minimizing collision risks.

Similar to the observations with stern deployment, Fig. 10 indicates

Table 9
The deployment strategies in traditional field production and the new procedure.

	Field production	New procedure
Environmental limit (m)	0.75, 1.0	0.75, 1.0
Deployment position	stern	stern
Horizontal distance (m)	2.0	1.0
Winch speed (m/s)	0.5	0.3

that snap loads occur when winch speed is abruptly halted during the recovery phase for ROV deployment from vessel side. In the descending phase, wire tension remains relatively stable; however, it evidently escalates with increased horizontal distance during the ascending phase. In Fig. 9(c), the maximum wire tension is approximately 2.4 times the weight of ROV. However, for ROV deployment from vessel side as shown in Fig. 10(c), it reaches about 3.1 times. Therefore, deploying the ROV from the side of the ship as shown in Fig. 10(c) results in slightly higher wire tension than deploying it from the stern at the same horizontal distance, as depicted in Fig. 9(c). This is attributed to the waves coming from the stern direction exerting less impact on the movement of the transverse radius of gyration.

4.2. Influence of winch speed

Optimizing winch speed selection is often a mean for minimizing sudden load occurrences during ROV operations. In a scenario where the ROV is deployed 2.0 m horizontally from the ship hull and other conditions are the same as in Fig. 10, numerical simulations were performed using three field-standard winch speeds appropriate for the small OSV in the case study. The results, showcasing the time history of wire tension, is illustrated in Fig. 11.

Due to identical winch start time and total travelling distance, the stop time of ROV varies with each speed, as presented in Fig. 11. The instantaneous wire tension escalates evidently during the recovery phase, as ROV moving at higher speeds exhibit increased inertia and acceleration. While higher winch speed is advantageous for descending the ROV, thereby shortening operation times, they have little effect on maximum wire tension during the launch phase. Conversely, adopting a lower winch speed of 0.3 m/s, as opposed to the conventional 0.5 m/s, for ascending phases significantly reduces maximum wire tension, enhancing operational safety.

4.3. Environmental limit of ROV operation

According to consultations with onboard operator of the OSV used in the case study, the current operational limit for ROV deployment in field operation is defined by a significant wave height of 1.0 m. In order to demonstrate the appropriateness of the current practice, as the first step, this study considers two significant wave heights, 0.75 m and 1.0 m, to reflect the existing operational threshold. The new procedure for ROV launch and recovery involves reductions in winch speed and horizontal distance, as detailed in Table 9. Fig. 12 illustrates a comparison of wire tension under traditional field operational conditions and the new procedure.

The maximum wire tension under the new procedure decreases slightly at a significant wave height of 0.75 m as shown in Fig. 12(a). However, under the significant wave height of 1.0 m, shown in Fig. 12 (b), the maximum wire tension during the recovery phase is halved, equivalent to a reduction of approximately 2.0 times the weight of ROV compared to traditional field operation. This substantial decrease in maximum wire tension underscores the effectiveness of the new procedure in enhancing both equipment and operational safety. The rated break strength of winch wire, 1.813 times the weight of ROV as listed in Table 4 and is exceeded by the maximum wire tension under traditional field operation strategies. However, the new procedure maintains maximum wire tension within safe limits under a significant wave height of 1.0 m, as evidenced in Fig. 12. To identify potential expansions of the ROV operational limit, the significant wave height is further increased, with findings presented in Fig. 13.

Under a significant wave height of 1.25 m, the maximum wire tension approaches but does not surpass the rated break strength of winch wire in Fig. 13(a). However, this threshold is exceeded at a wave height

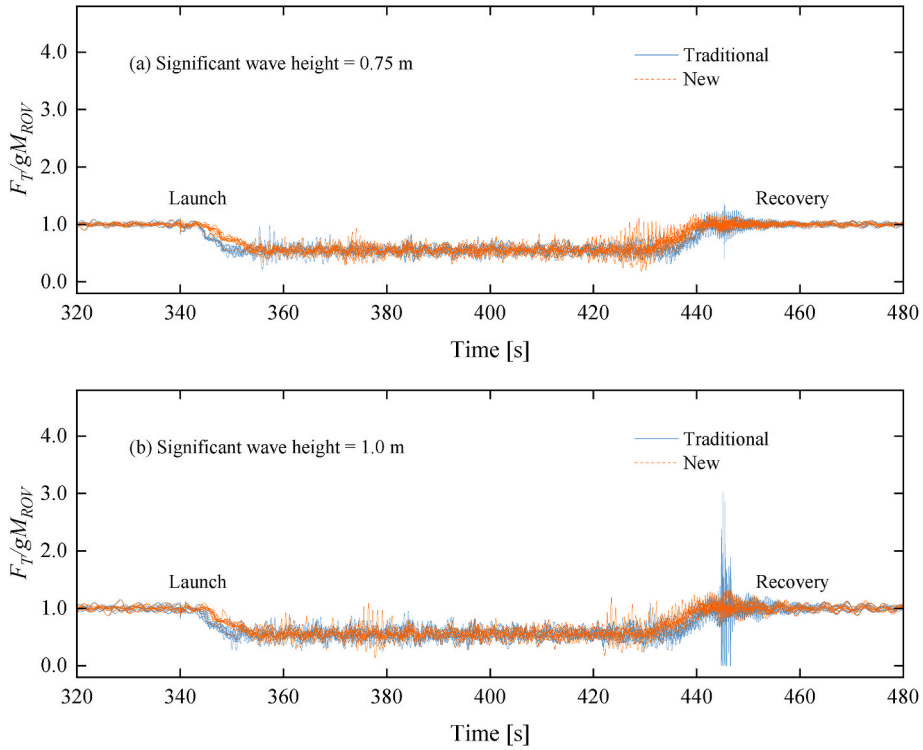

Fig. 12. Comparison of time history of wire tension between traditional and new strategies under environmental limits when ROV deployment from vessel stern.

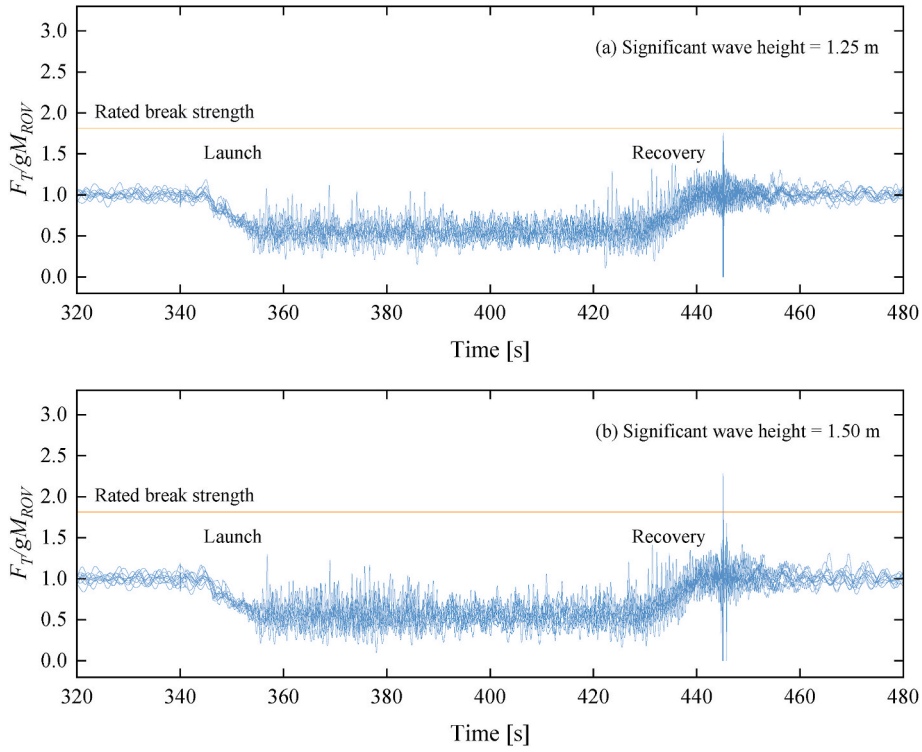

Fig. 13. The environmental limit for ROV operation under new strategies when deployment from vessel stern.

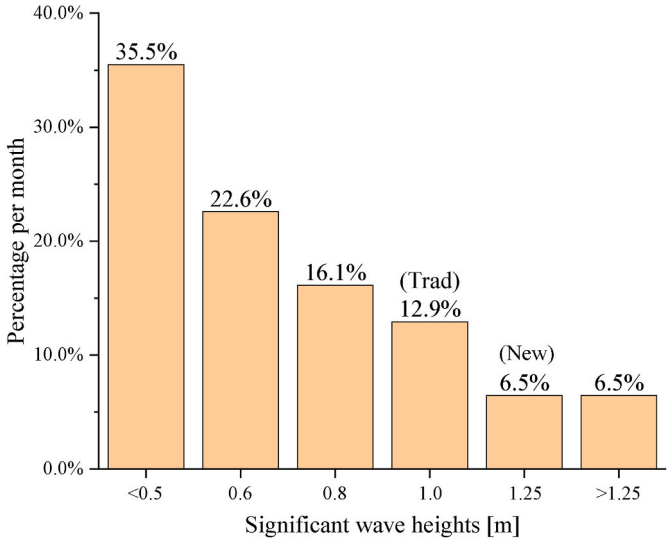

Fig. 14. The statistics of significant wave heights at the DanTysk wind farm from StormGeo weather forecast.

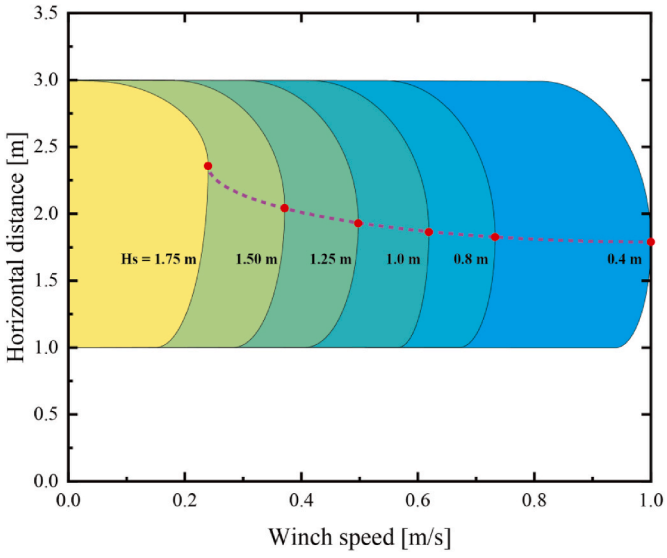

Fig. 15. Safe operating envelope of ROV deployment from vessel stern under three primary environmental and operational parameters: significant wave height, winch speed, horizontal distance of ROV to the vessel hull.

of 1.50 m, as shown in Fig. 13(b). Consequently, the new procedure potentially elevates the operational limit for ROV deployment in field operation to a significant wave height of 1.50 m.

4.4. Expansion of operational capacity

Expanding operational capacity through improved ROV deployment strategies is further examined based on comprehensive numerical simulation. Fig. 14 presents the statistics of significant wave heights at the DanTysk wind farm in May 2020 (31 days), sourced from StormGeo weather forecasts. As mentioned above, the operational limit is 1.0 m using the traditional methods, denoted as Trad, whereas the operational limit under the new strategy is 1.25 m, denoted as New. Under the conventional ROV launch and recovery procedures, 27 days (87.1%, 0–1.0 m significant wave height) per month typically align with the criteria for safe operations. However, with the implementation of the new safety guidelines developed in the present for ROV operation, an additional two operating windows (6.5%, 1.25 m significant wave height) per month are anticipated. Assuming this month is representative, the annual increase in operational windows is estimated to be approximately 6.5%.

4.5. Safe operating envelope

The safe operating envelope of ROV deployment onboard a small OSV in the new procedure is defined as: 1) the maximum tension in winch wire does not exceed its rated break strength and 2) the maximum tension in mooring lines does not exceed the rated break strength. Given the variability of surface wave conditions, which can differ at any given moment or location even within the same significant wave height and peak period due to the stochastic nature of wave patterns, the present numerical simulations are carried out for 10 operating cycles for each wave condition using different wave seeds. This approach was taken to achieve statistical reliability and an accurate assessment of wire tension. The outcomes of these simulations are depicted in Fig. 15.

The maximum horizontal distance 3.0 m is based on the limit of crane boom length of the OSV, Fortuna Kingfisher for the present case study, and the minimum is 1.0 m to ensure that the ROV avoids collision with the vessel hull during the operation. The winch speed is typically less than 1.0 m/s to avoid the excessive impact on winch wire as described previously. The critical curve (dotted line) that satisfies the definition of safe operating envelope of ROV deployment on vessel stern at maximum winch speed is shown in Fig. 15. The curves corresponding to each significant wave height represent the combined critical values for safe ROV deployment. The significant wave height of 1.75 m is considered the most extreme sea state for the small OSV in the present study, while Fig. 15 shows that it is safe for ROV deployment across the whole range of the winch speed up to 1.0 m/s and the horizontal distance between 1 m to 3 m under the significant wave height less than 0.4 m. The dashed line intercepts with the curve of a significant wave height of 0.4 m representing the condition under which a maximum winch speed of 1.0 m/s can be used. The area enclosed by the curve represents the range of horizontal distance and winch speed under which the ROV can be safely operated under the sea state with the significant wave height. As environmental conditions become more severe with increased significant wave height, the enclosed area of the curve is markedly reduced indicating considerable restriction for safe operation towards lower winch speed with the set horizontal distance. The maximum winch speed can be safely operated for each given sea state is seen initially increases and then decreases as the deployment position of ROV gradually moves away from the vessel hull. The critical values shown as red dot points in Fig. 15 reveal a combination of the maximum winch speed can be safely operated with the corresponding horizontal distance under the given sea state (significant wave height). The dotted curve in purple is formed by connecting the critical points in each sea state, representing the maximum winch speed the ROV can be safely operated at the horizontal distance under the given sea state. Fig. 15 provides a simple, straightforward guidance for onboard safe ROV operation crucial for the small OSV currently operating widely for offshore wind farms O&M in European waters. This is a significant step forward in improving the ROV safe operation from empirical onboard staff experience-based towards science/technology-based practice. The chart can also be used for potential capability extension of the OSV operation.

5. Conclusions

The deployment of a work class ROV from the small offshore service vessel based on single point mooring system method is studied in this paper. The effect of winch speed and deployment position on the wire tension during launch and recovery process of ROV is investigated based on numerical simulation. The developed numerical model is validated against experimental results of calm water and regular waves on a 1:10 scaled model in a wave flume, as well as previous numerical study focused on single point mooring system. The StormGeo weather forecast data at the DanTysk wind farm in May 2020 is used to simulate realistic operating sea state and analyse operational capacity.

The safety of ROV deployment is found to be more critical in recovery process than in launch process. Higher winch speed can be used for descending ROV to reduce the operational time, but a lower winch speed for ascending is beneficial to reduce the maximum wire tension. The increase of horizontal distance has a little effect on the wire tension during launch phase. However, the maximum wire tension decreased with the decrease of horizontal distance in recovery stage. The horizontal distance has little influence on the probability of sudden loading, and its main influencing factor is the significant wave height.

With the deployment position at the stern, a horizontal distance of 1.0 m, and a winch speed of 0.3 m/s, the new safety strategy can reduce maximum wire tension effectively, and the ROV operational limit is expanded to a significant wave height of 1.25 m based on the improvement measures. The operational capacity of ROV can be expanded by up to 6.5% annually while ensuring safety of deployment operation.

The safe operating envelope of ROV deployment is proposed based on the comprehensive numerical simulation to guide the onboard ROV safe operation of winch speed and horizontal distance under given sea state. It is a significant step forward in improving the ROV safe operation from empirical onboard staff experience-based towards science/technology-based practice. The chart can also be used for potential capability extension of the OSV operation.

CRediT authorship contribution statement

Yulin Deng: Writing – review & editing, Writing – original draft, Validation, Project administration, Methodology, Investigation, Formal analysis. **Xiudi Ren:** Investigation, Data curation. **Martin Nuernberg:** Writing – review & editing, Resources, Methodology, Data curation. **Longbin Tao:** Writing – review & editing, Writing – original draft, Supervision, Software, Resources, Project administration, Methodology, Investigation, Funding acquisition, Data curation, Conceptualization.

Declaration of competing interest

The authors declare that they have no known competing financial interests or personal relationships that could have appeared to influence the work reported in this paper.

References

Bjerkholt, R.F., 2014. Analysis of ROV Lift Operation.
de Andrade, E.M., de Oliveira Costa, D., Fernandes, A.C., Junior, J.S.S., 2023. A review on the modeling of subsea lifting operations. Ocean Eng. 268, 113293.
DNV, 2019. In: Modelling and Analysis of Marine Operations, DNVGL-RP-N103. Det Norske Veritas, Norway.
Driscoll, F.R., Lueck, R.G., Nahon, M.J.A.O.R., 2000. Development and validation of a lumped-mass dynamics model of a deep-sea ROV system. Appl. Ocean Res. 22 (3), 169–182.
Feng, Z., Allen, R., 2004. Evaluation of the effects of the communication cable on the dynamics of an underwater flight vehicle. Ocean Eng. 31 (8–9), 1019–1035.
Hennessey, C.M., Pearson, N.J., Plaut, R.H., 2005. Experimental snap loading of synthetic ropes. Shock Vib. 12 (3), 163–175.
Hsu, W.T., Thiagarajan, K.P., Manuel, L., 2017. Extreme mooring tensions due to snap loads on a floating offshore wind turbine system. Mar. Struct. 55, 182–199.
Jenssen, F.R., 2015. Dynamic Analysis of ROV Operation.
Kimiaei, M., Xu, J., Yu, H., 2009. Comparing the results of a simplified numerical model with DNV guidelines for installation of subsea platforms. Int. Conf. Offshore Mech. Arctic Eng. 43413, 319–326.
Lubis, B., 2021. Structural Response Analysis for Launch, Recovery, and Operation of an Ultra-deep-water Work Class Remotely Operated Vehicle under Ocean Current and Wave. Doctoral dissertation, The University of Western Australia.
Lubis, M.B., Kimiaei, M., 2021. Wave flume and numerical test on launch and recovery of ultra-deep-water ROV through splash zone under wave and ship motion. Ocean Eng. 238, 109767.
Nuernberg, M., Tao, L., Ren, X., Ramzanpoor, I., 2021. Single point mooring for subsea inspections of wind turbine foundations. Energy Technology Partnership (ETP) project report. pp. 5-7.
Øritsland, O., 1989. A summary of subsea module hydrodynamic data. Marine Operations - Crane Operations.
Ren, X., Tao, L., Nuernberg, M., Ramzanpoor, I., 2022. Interaction of offshore support vessel with adjacent offshore wind turbine during maintenance operation. In: International Conference on Offshore Mechanics and Arctic Engineering, vol. 85932. American Society of Mechanical Engineers, V008T09A027.

Sayer, P., 2008. Hydrodynamic loads during the deployment of ROVs. Ocean Eng. 35 (1), 41–46.
SINTEF Ocean, 2022. Documentation for SIMO. Version 4.4.0. Retrieved from. https://sima.sintef.no/doc/4.4.0/simo/index.html.
Valen, M., 2010. Launch and Recovery of ROV: Investigation of Operational Limit from DNV Recommended Practices and Time Domain Simulations in SIMO.